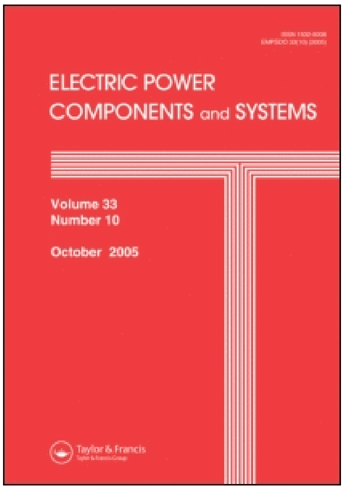

Electric Power Components and Systems
Publication details, including instructions for authors and subscription information:
http://www.informaworld.com/smpp/title~content=t713399721

Generalized Regression Neural-network-based Modeling Approach for Traveling-wave Ultrasonic Motors

Tien-Chi Chen [a]; Chih-Hsien Yu [b]
[a] Department of Electrical Engineering and Department of Electro-Optical Engineering, Kun Shan University, Tainan, Taiwan [b] Department of Engineering Science, National Cheng Kung University, Tainan, Taiwan

Online Publication Date: 01 June 2009

To cite this Article Chen, Tien-Chi and Yu, Chih-Hsien(2009)'Generalized Regression Neural-network-based Modeling Approach for Traveling-wave Ultrasonic Motors',Electric Power Components and Systems,37:6,645 — 657

To link to this Article: DOI: 10.1080/15325000802705612

URL: http://dx.doi.org/10.1080/15325000802705612

Electric Power Components and Systems, 37:645–657, 2009

ISSN: 1532-5008 print/1532-5016 online
DOI: 10.1080/15325000802705612

Taylor & Francis
Taylor & Francis Group

Generalized Regression Neural-network-based Modeling Approach for Traveling-wave Ultrasonic Motors

TIEN-CHI CHEN[1] and CHIH-HSIEN YU[2]

[1]Department of Electrical Engineering and Department of Electro-Optical Engineering, Kun Shan University, Tainan, Taiwan
[2]Department of Engineering Science, National Cheng Kung University, Tainan, Taiwan

Abstract *As the dynamic characteristics of the traveling-wave ultrasonic motor are highly non-linear and time varying, an analysis model is difficult to obtain. It is difficult to design a suitable controller to achieve high-precision position control using conventional control techniques. A new identification approach is proposed and implemented, and it aims to provide a practical model for controller design and simulation. As a result, a generalized regression neural-network-based model is developed to identify the relation between input excited frequency and phase difference of two-phase AC voltages and the output driving torque generated by the traveling-wave ultrasonic motor. One major advantage is that transfer function identification is no longer required. The other advantage is that it allows for the application of traditional controller design and standard software simulation.*

Keywords traveling wave ultrasonic motor, generalized regression neural network

1. Introduction

The traveling-wave ultrasonic motor (TWUSM) has excellent performance and many useful features such as high holding torque, high torque at low speed, quiet operation (ultrasonic), simple structure, compact size, and no electromagnetic interferences. However, the mathematical model of the ultrasonic motor (USM) is complex and difficult to derive due to its driving principle, which is based on high-frequency mechanical vibrations and frictional force [1]. Despite many attempts, a lumped motor model of the USM is unavailable so far. The dynamical characteristics of the USM are complicated and highly non-linear, and the motor parameters are time varying due to temperature rise and changes in motor drive operating conditions. Therefore, it is difficult to predict the performance characteristics of the USM under various working conditions.

Received 29 July 2008; accepted 12 December 2008.
Address correspondence to Prof. Tien-Chi Chen, Department of Electrical Engineering, Kun Shan University, No. 949 Da Wan Road, Yung-Kang City, Tainan Hsien, 710, Taiwan, R.O.C. E-mail: tchichen@mail.ncku.edu.tw

These dynamics contain many complicated and non-linear characteristics that depend on load torque, driving frequency, applied voltages, operating temperature, and static pressure force between the stator and rotor of the USM. The main sources of the non-linearities in the USM dynamics are the non-linearity dead-zone and the saturation reverse effect; both of them vary as the driving conditions change. Therefore, despite many reported attempts [2, 3], the modeling of this device is still a challenging problem.

There has been considerable attention over the years on research using the neural network (NN)-based control technique when solving control problems. Many authors have suggested NNs as powerful building blocks for a wide class of complex non-linear system control strategies when no complete model information exists or when a controlled plant is considered a "black box."

A comprehensive survey on NN control can be founded in [4]. The most useful property of a generalized regression neural network (GRNN) in control is its ability to uniformly approximate arbitrary input–output linear or non-linear mappings. Based on this property, the GRNN-based model has been developed to identify the effects of non-linearities and system uncertainties in TWUSM drive system.

The application of the GRNN is not only for control problems but also for model-free function approximation. It has already been validated that the GRNN can approximate a non-linear function over a domain of interest to any desired accuracy. Furthermore, this model constitutes a powerful and suitable test bench for the control community for investigating the usability of the existing linear and non-linear control methods in a simulated environment. Consequently, the existing control algorithms can be applied directly to the simulated model, and thereby, their degree of usability and performance can be established without resorting to actual experiments. Moreover, this model provides the opportunity for the control community to push their knowledge forward, thereby finding new, more suitable methods for controlling these kinds of devices.

In this article, a GRNN-based model structure is adopted that is based on experimental measurements obtained for different conditions on load torques, driving frequency, and input phase differences. The developed model is a simplified one that is suitable for control design purposes. The main aim of this article is to develop a GRNN-based model system for identifying the non-linearity of TWUSM drive system with a dead-zone.

2. GRNN

The GRNN is an NN architecture that can solve any function approximation problem. The GRNN proposed by Specht [5] does not require an iterative training procedure. It approximates any arbitrary function between input and output vectors, drawing the function estimate directly from the training data. In addition, it is consistent that as the training set size becomes large, the estimation error approaches zero. The GRNN is used for the estimation of continuous variables, as in standard regression techniques. It is related to the radial basis function network and is based on a standard statistical technique called kernel regression. By definition, the regression of a dependent variable y on an independent x estimates the most probable value for y, given x and a training set. The regression method will produce the estimated value of y, which minimizes the mean-squared error (MSE). The principal advantages of the GRNN are its fast learning and convergence to the optimal regression surface as the number of samples becomes very large. The GRNN is particularly advantageous with sparse data in a real-time environment

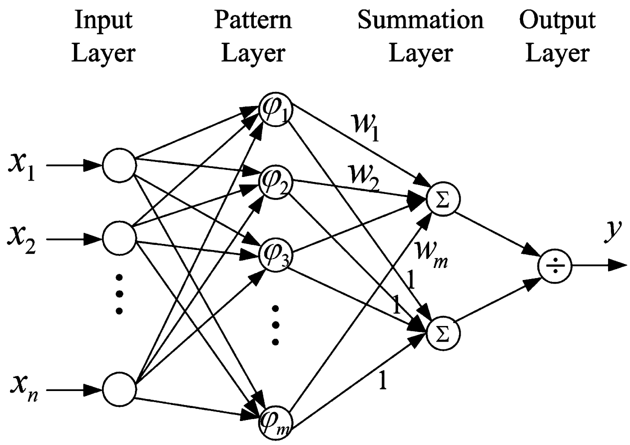

Figure 1. Schematic diagram of GRNN architecture.

because the regression surface is instantly defined everywhere. The schematic diagram of GRNN architecture is presented in Figure 1.

As seen in Figure 1, the GRNN is organized using an input layer, a pattern layer, a summation layer, and an output layer. The relation between input and output can be expressed as

$$y = \frac{\sum_{j=1}^{m} w_j \varphi_j(X)}{\sum_{j=1}^{m} \varphi_j(X)} \equiv \frac{\alpha}{\beta}, \tag{1}$$

where $X = [x_1, x_2, \ldots, x_n]^T$ is an n-dimensional input vector, w_j is the weight between the jth pattern layer node and the summation layer node, and φ is the Gaussian function.

Layer 1, the input layer, accepts the input signals into the GRNN. The nodes at layer 1 represent linguistic variables (namely, the driving frequency f and the phase difference ϕ in the TWUSM drive system [6]). Layer 2, the pattern layer, possesses a non-linear transformation applied on the data from the input space to the pattern space. The most popular choice for the function φ is a multivariate Gaussian function with an appropriate mean and autocovariance matrix. The Gaussian function is

$$\varphi_j(X) = \exp\left(-\frac{\|X - C_j\|^2}{\delta_j^2}\right) = \prod_{i=1}^{n} \exp\left[-\left(\frac{x_i - \overline{x}_i^j}{\delta_j}\right)^2\right], \tag{2}$$

where $C_j = [\overline{x}_1^j, \overline{x}_2^j, \ldots, \overline{x}_n^j]^T$ and δ_j are the center vector and the standard deviation of the Gaussian function, respectively.

Layer 3, the summation layer, executes the sum operation in Eq. (1). The outputs of the pattern layer nodes are multiplied with appropriate interconnection weights to sum up for producing the output of the network. Layer 4 is the output layer, where the nodes are represented by a GRNN individual output.

3. Modeling of TWUSM Drive System

To obtain a practical model for control design purposes, a specific USM (*i.e.*, the USR-60 [Shinsei, Japan]) was studied. Figure 2 shows the actual configuration view of a typical USR-60 circular traveling-wave type motor, in which the specification is a 40-kHz, 0.32-Nm, 3-W, 120-rev/min type motor. The operation of a mode conversion USM is based on the torque generated by piezoelectric ultrasonic vibrations. An optimal supply voltage for the USM is a sinusoidal voltage with frequency near the mechanical resonance frequency of the stator-rotor assembly. Since this USM presents a large capacitive load and requires a high operating frequency (40 kHz), its equivalent impedance could be extremely low. This USM also requires a high drive voltage (400 V peak-to-peak), which leads to a large drive current.

The goals for drive circuit design are to satisfy these requirements as well as achieve high power efficiency and reduce the system hardware size and cost. In the design of a modern drive circuit with an adjustable phase difference, the key technology is a low-cost and simple phase shifter circuit that provides two-phase signals from a two-phase voltage source. The purpose of this study is to design a novel driving scheme that simultaneously employs both the driving frequency and phase difference as the dual-mode control variables to handle system non-linearities and parameter variations. The block diagram of the driving circuit and the design procedures of the proposed drive system are described in [6, 7].

From [7], it is clear that the highest speed is achieved for a temporal phase shift of $+90°$ or $-90°$, which indicates that the two phases fulfill the symmetry requirements for a perfect traveling-wave generation. The motor can also be made to rotate in the forward/backward direction and to stop smoothly by controlling the phase difference. This is why the phase difference of the applied voltages is usually chosen as the actuating variable in the position control applications of the motor. The speed characteristics for

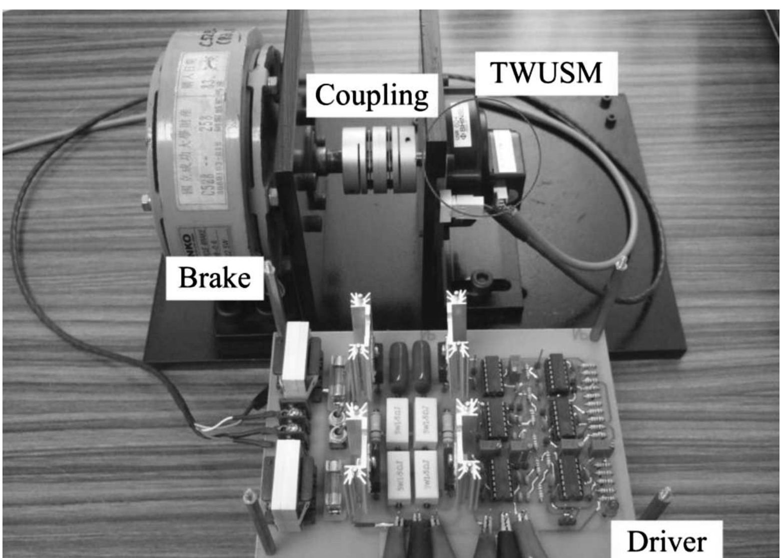

Figure 2. Photograph of experimental setup.

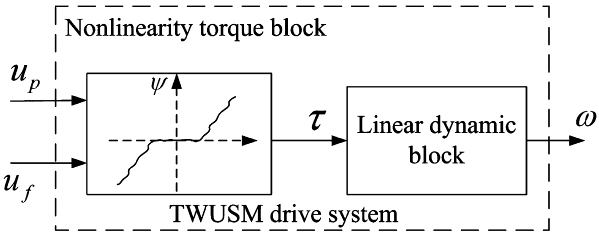

Figure 3. A class of non-linear TWUSM drive system.

the phase difference hold heavy non-linearity. As it is seen, variation of this dead-zone width with applied driving frequency is experimentally determined. It can be noticed that the dead-zone varies almost unmethodically with the excitation frequency and exhibits different behavior in forward and backward directions. These dynamics contain many complicated and non-linear characteristics that depend on load torque, driving frequency, applied voltages, operating temperature, and static pressure force between the stator and rotor of the TWUSM. Deriving a mathematical model for representing the TWUSM dynamic is not a very simple task.

A general class of control systems with unknown dead-zone non-linearity can be divided into a series of connections of a non-linear (dead-zone) subsystem and a linear time invariant plant. The TWUSM drive system model consists of a static non-linear block in series with a dynamic linear block, as shown in Figure 3. Figure 3 shows a hypothetical, non-symmetric dead-zone non-linearity ψ, dependent on driving frequency and phase difference control of applied two-phase AC driving voltages in the TWUSM drive circuit. In this case, u_p, u_f, and τ are the phase-modulated and frequency-modulated control signals in the driving system and the actuator driving torque output. By the driving experimental results in [7], it is assumed that the actuator driving torque has a non-linear dead-zone form, which is more general and sensible.

3.1. Dead-zone Non-linearity

Figure 4 shows a non-symmetric dead-zone non-linearity $\psi(u_p)$, where u_p and τ are scalars. In this case, u_p and τ are the phase-modulated control signal in the drive

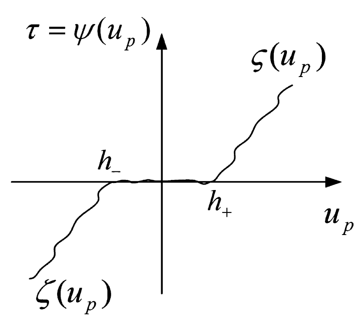

Figure 4. Non-symmetric dead-zone non-linearity of TWUSM drive system under a fixed excitation frequency.

system and the actuator driving torque output, respectively. By according to the driving experimental results in [7], it is assumed that the actuator driving torque has a non-linear dead-zone form, which is more general and sensible. A mathematical model for the dead-zone characteristic of Figure 4 is given by

$$\tau = \psi(u_p) = \begin{cases} \zeta(u_p) < 0, & u_p \le h_- \\ 0, & -h_- < u_p < h_+ \\ \varsigma(u_p) > 0, & u \ge h_+ \end{cases}, \tag{3}$$

where the functions $\zeta(u_p)$ and $\varsigma(u_p)$ are smooth, non-linear functions, so this describes a very general class of $\psi(u_p)$. All of $\zeta(u_p)$, $\varsigma(u_p)$, h_-, and h_+ are unknown, so that it is more general and sensible.

3.2. *Identification of the TWUSM Drive System Using GRNN*

In this section, a GRNN estimator for identifying the non-linearity dead-zone of a TWUSM drive system is given. It is not required to be symmetrical, and the function outside the dead-band may not be a linear function. The proposed method can be applied for the identification of any bounded, unknown, non-linear function. The generality of the method and applicability to a broad range of non-linear functions make this approach a potentially useful tool under backlash, hysteresis, and other non-linearities. Besides the above discussion, like other motors, the TWUSM's rotor motion exhibits dynamic behavior that can be represented by the following equation [8, 9]:

$$\tau(t) = J\frac{d\omega(t)}{dt} + B\omega(t) + \tau_L(t), \tag{4}$$

where J and B denote the moment of inertia and viscous coefficients, and τ_L is the external force disturbance. For the linear dynamic equation of Eq. (4), the dynamics of the TWUSM's rotor can be expressed as

$$\omega(k) = \sum_{i=1}^{n} a_i\omega(k-i) + \sum_{j=0}^{n-1} b_j\tau(k-j), \tag{5}$$

where a_i and b_j are coefficients of the system, and n is an order of the system.

The identification network for the non-linear torque block and linear dynamic block is illustrated in Figure 5. The input signal ($X(k) = [x_1(k)\ \ x_2(k)] \equiv [\phi\ \ f]$) gets into

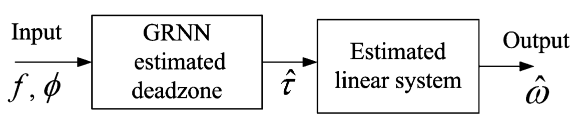

Figure 5. Block diagram of GRNN-based model for TWUSM.

the GRNN to identify the actuator driving torque output, while the output signal ($\hat{\tau}$) together with the previous output signal ($\omega(k-1), \ldots, \omega(k-n)$) are used to identify the parameter of the linear dynamic system by a single-layer network, as shown in Figure 6. The relation between $X(k)$ and $\hat{\tau}(k)$ can be described as

$$\hat{\tau}(k) = \frac{\sum_{j=1}^{m} w_j \varphi_j(X(k))}{\sum_{j=1}^{m} \varphi_j(X(k))}. \tag{6}$$

According to Eqs. (5) and (6), the identification network output is given by

$$\hat{\omega}(k) = \sum_{i=1}^{n} a_i \omega(k-i) + b_0 \left(\frac{\sum_{j=1}^{m} w_j \varphi_j(X(k))}{\sum_{j=1}^{m} \varphi_j(X(k))} \right) + \sum_{i=1}^{n-1} b_i \hat{\tau}(k-i), \tag{7}$$

where n is the order of the linear system, and m is the number of hidden layer of GRNNs. Equation (7) can be rewritten in a matrix form as

$$\hat{\omega}(k) = W_n X_n(k), \tag{8}$$

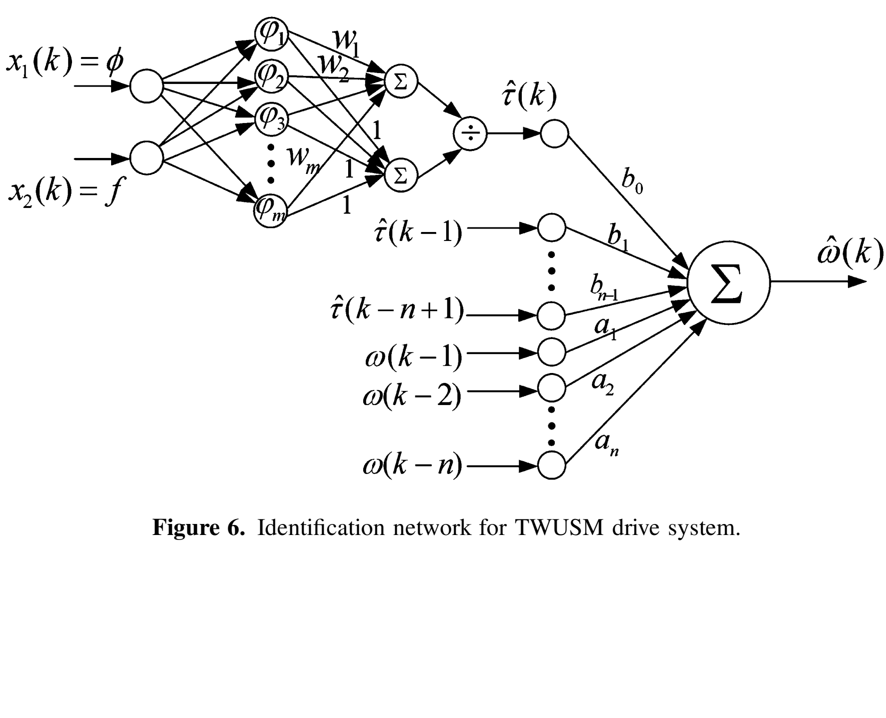

Figure 6. Identification network for TWUSM drive system.

where $W_n = [a_1, a_2, \ldots, a_n, b_0 w_1, b_0 w_2, \ldots, b_0 w_m, b_1, \ldots, b_{n-1}]$ is the weight vector of the single hidden-layer network and the GRNN. The input vector of the network is

$$X_n = \left[\omega(k-1), \ldots, \omega(k-n), \frac{\varphi_1(X(k))}{\sum_{j=1}^{m} \varphi_j(X(k))}, \ldots, \frac{\varphi_m(X(k))}{\sum_{j=1}^{m} \varphi_j(X(k))}, \hat{\tau}(k-1), \ldots, \hat{\tau}(k-n+1) \right]. \tag{9}$$

If C_j and δ_j are chosen, $\varphi_j(X(k))$ can be obtained by computing the Gaussian function in Eq. (2). For network training, a conventional cost function is defined by

$$E_\omega(k) = \frac{e_\omega^2(k)}{2}, \tag{10}$$

where $e_\omega(k) = \hat{\omega}(k) - \omega(k)$. The weighting factors of the identification network is updated by a gradient descent algorithm that can be expressed as the following form:

$$W_n(k+1) = W_n(k) - \eta(k) \frac{\partial E_\omega(k)}{\partial W_n(k)} = W_n(k) - \eta(k) e_\omega X_n(k), \tag{11}$$

where $\eta(k)$ is a learning rate of the identification network. The convergence of Eq. (11) can be ensured by the Lyapunov stability theory [10]. If $\omega(k) = W_n^* X_n(k)$, then the error function becomes

$$e_\omega(k) = W_n(k) X_n(k) - W_n^* X_n(k) = \overline{W}_n(k) X_n(k). \tag{12}$$

From Eq. (11), we have

$$\overline{W}_n(k+1) = \overline{W}_n(k) - \eta(k) e_\omega(k) X_n(k). \tag{13}$$

To prove the convergence, we define a positive definite Lyapunov function $V(k) = \|\overline{W}_n(k)\|^2$. From Eq. (13), we have

$$\begin{aligned} \Delta V(k+1) &= V(k+1) - V(k) = \|\overline{W}_n(k+1)\|^2 - \|\overline{W}_n(k)\|^2 \\ &= \eta(k)^2 |e_\omega(k)|^2 \|X_n(k)\|^2 - 2\eta(k) tr\{e_\omega(k) X_n(k)^T \overline{W}_n(k)^T\}. \end{aligned} \tag{14}$$

Identifying $tr\{AB\} = tr\{BA\}$ and $tr\{X_n(k)^T \overline{W}_n(k)^T e_\omega(k)\} = tr\{e_\omega^T(k) e_\omega(k)\}$, we can get following form by using the norm properties:

$$\Delta V(k+1) = -\eta(k)\lfloor 2e_\omega^2(k) - \eta(k)\|X_n(k)\|^2 e_\omega^2(k)\rfloor \tag{15}$$

$$= -\eta(k)\lfloor 2 - \eta(k)\|X_n(k)\|^2\rfloor e_\omega^2(k).$$

This implies that if $0 < \eta(k) < 2/\|X_n\|^2$, the convergence of training is ensured.

4. Simulations and Model Validation

The derived GRNN model of the TWUSM is implemented in a Matlab software environment. The results achieved by the simulated model are then compared to measured characteristics in order to establish the validity of the model.

The performance of the simulated model is given in terms of the output speed performance under varying frequency and phase difference. The range of frequencies between 41 kHz and 43 kHz is explored, and the achieved results are given in Figures 7–9. It must be emphasized that the results reposted in this figure are obtained for the free motor (*i.e.*, no load) operating under its nominal conditions. Also in Figures 7–9, the results of real speed measured directly on the motor are reported. It can be seen that there is agreement between the simulated model and the measured data, which validated the proposed modeling of the TWUSM drive system.

The speed-torque relationship is the most important characteristic of any electromechanical motor, and therefore, model validation should respect this criterion. Figure 10 represents speed-frequency characteristics under different load torques obtained from the

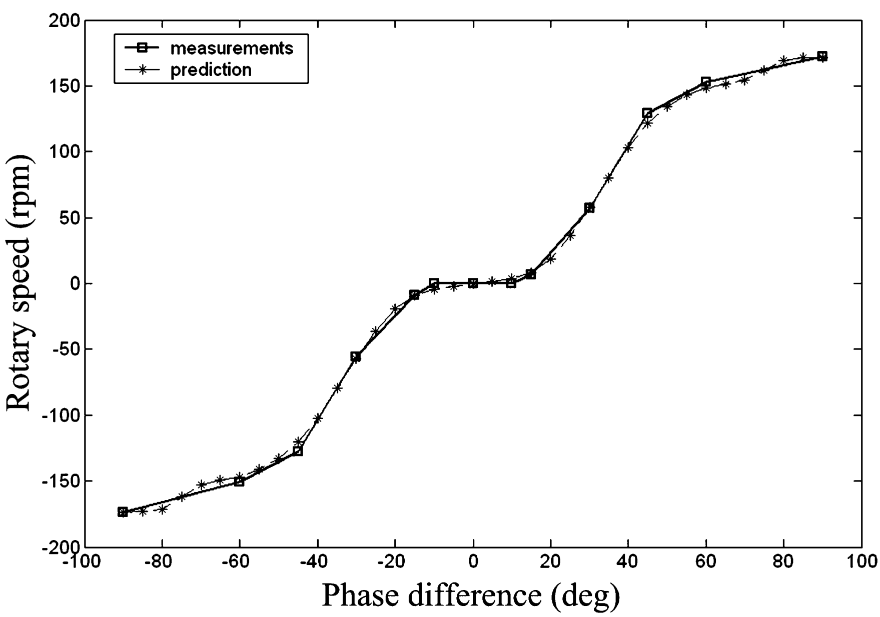

Figure 7. Comparison of the rotary speed phase shift characteristics at the driving frequency 41 kHz: simulation and measurements.

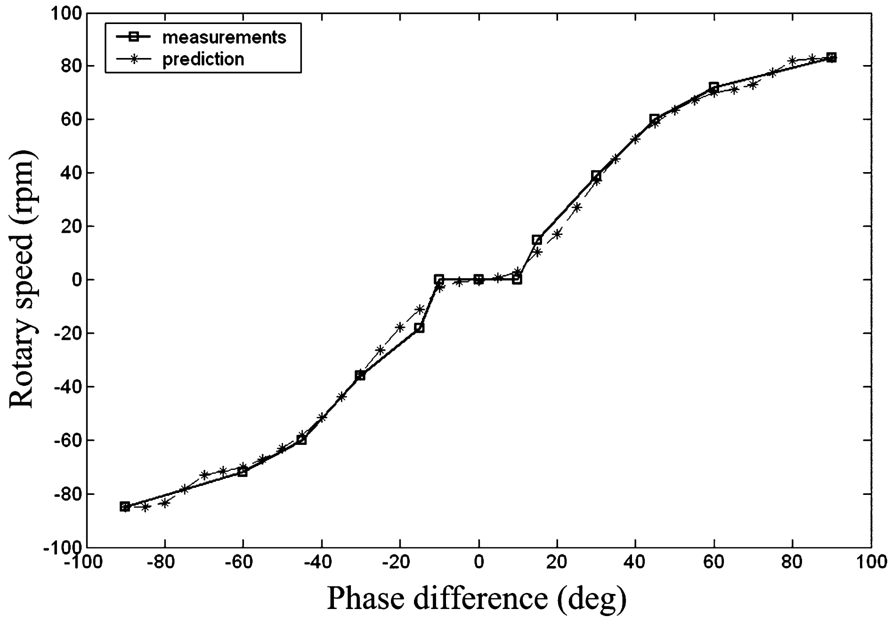

Figure 8. Comparison of the rotary speed phase shift characteristics at the driving frequency 42 kHz: simulation and measurements.

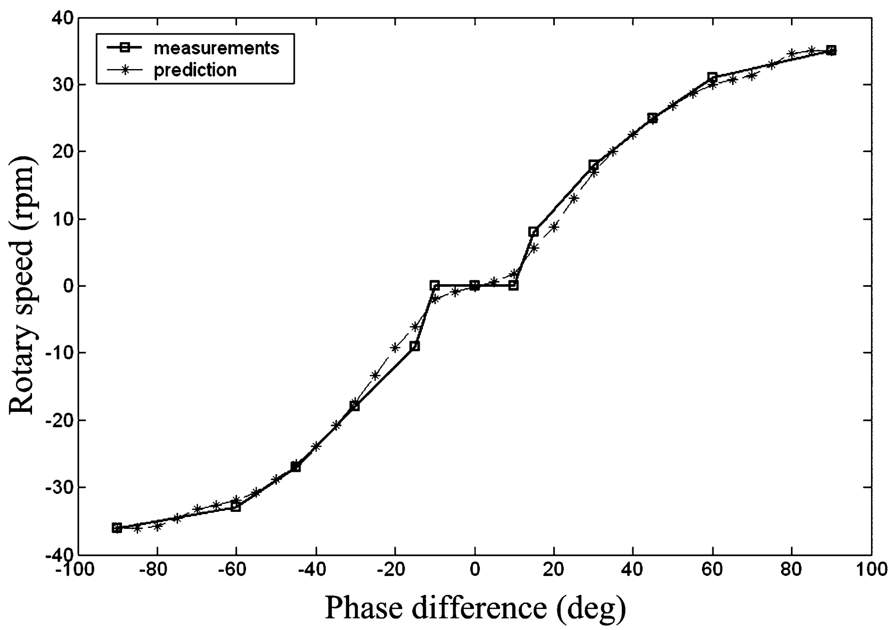

Figure 9. Comparison of the rotary speed phase shift characteristics at the driving frequency 43 kHz: simulation and measurements.

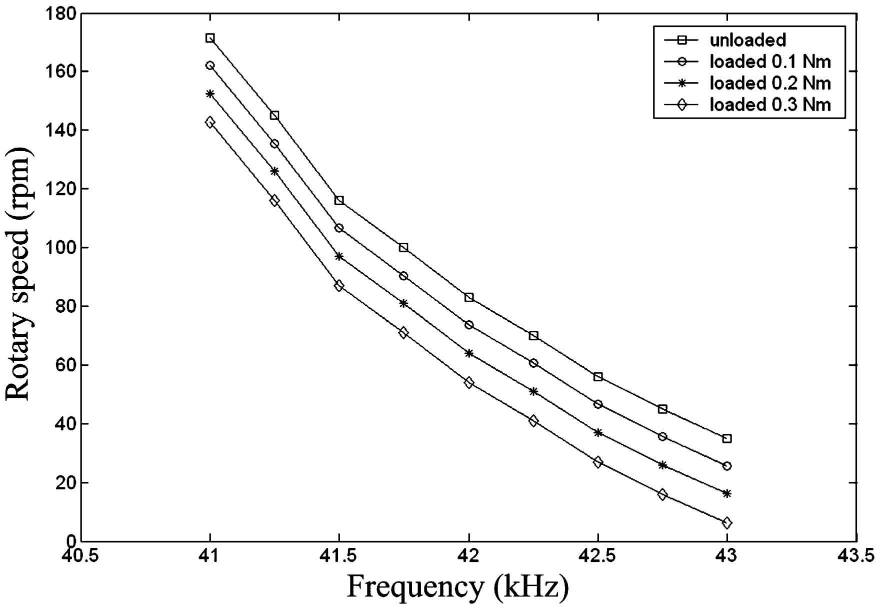

Figure 10. Prediction of speed-frequency characteristics at various load torques.

simulated model. The range of torque between 0 Nm and 0.3 Nm is explored, and the results achieved by the simulated model when compared to the real measurements are reported in Figure 11 for the load torques 0.1 Nm, 0.2 Nm, and 0.3 Nm, respectively. It can be noticed from the compared results that there is agreement between the simulated results and the measured results, which validates the model in the range of torques between 0 Nm and 0.3 Nm and frequencies of interest (*i.e.*, in the neighborhood above the fundamental resonance frequency).

5. Conclusions

This article considers the modeling of a TWUSM drive system, with the emphasis on the procedure of deriving a simplified and practical model with low computational demands. The USMs possess heavy non-linear and load-dependent characteristics such as dead-zone and saturation reverse effects, which vary with driving conditions. A GRNN-based dead-zone estimator technique was presented for a class of non-linear TWUSM drive systems. Finally, the derived model has been simulated in a Matlab software environment to verify the validity of the model.

It must be emphasized that considering the experimental investigations, frequency/phase control is the most appropriate method for controlling the TWUSM. Therefore, a simple model representing the frequency/phase-output relationship must be derived from the GRNN-based architecture in order to design the control system for providing a simulated environment. Consequently, the existing control algorithms can be applied directly to the simulated model, and thereby, their degree of usability and performance can be established without resorting to actual experiments.

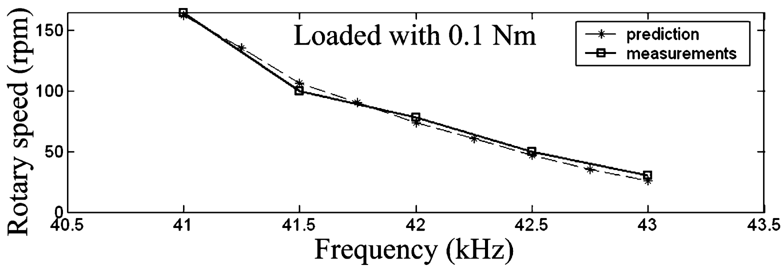

(a)

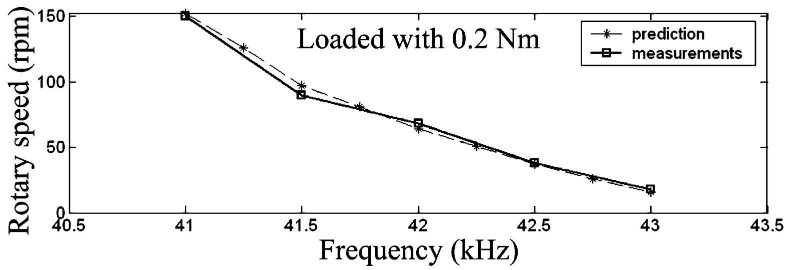

(b)

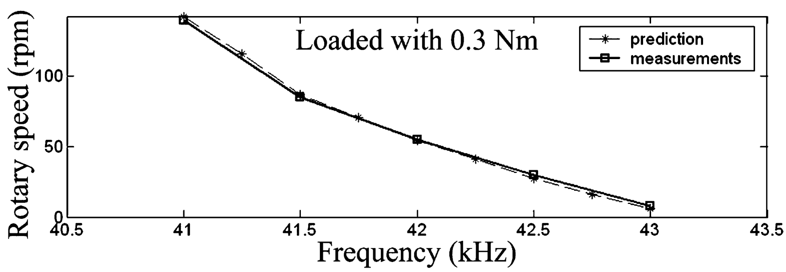

(c)

Figure 11. Comparison of the rotary speed frequency characteristics, simulation and measurements, at load torque: (a) 0.1 Nm, (b) 0.2 Nm, and (c) 0.3 Nm.

References

1. Sashida, T., and Kenjo, T., *An Introduction to Ultrasonic Motors*, Oxford: Oxford Science Publications, 1993.
2. Senjyu, T., Nakamura, M., Urasaki, N., Sekine, H., and Funabashi, T., "Mathematical model of ultrasonic motors for speed control," *Elect. Power Comp. Syst.*, Vol. 36, No. 6, pp. 637–648, 2008.
3. Zhang, X. L., and Tan, Y. H., "Modeling of ultrasonic motor with dead-zone based on Hammerstein model structure," *J. Zhejiang Univ. Sci. A*, Vol. 9, No. 1, pp. 58–64, 2008.
4. Hagan, M. T., Demuth, H. B., and Jesus, O. D., "An introduction to the use of neural networks in control systems," *Inter. J. Robust Nonlinear Control*, Vol. 12, No. 11, pp. 959–981, 2002.
5. Specht, D. F., "A general regression neural network," *IEEE Trans. Neural Networks*, Vol. 2, No. 6, pp. 568–576, 1991.

6. Chen, T. C., Yu, C. H., and Tsai, M. C., "A novel driver with adjustable frequency and phase for traveling-wave type ultrasonic motor," *J. Chinese Inst. Eng.*, Vol. 31, No. 4, pp. 709–713, 2008.
7. Chen, T. C., Yu, C. H., Chen, C. J., and Tsai, M. C., "Neuro-fuzzy speed control of traveling-wave type ultrasonic motor drive using frequency and phase modulation," *ISA Trans.*, Vol. 47, No. 3, pp. 325–338, 2008.
8. Chung, S. W., and Chau, K. T., "Speed control of traveling-wave ultrasonic motors using a practical modeling approach," *Elec. Power Comp. Syst.*, Vol. 35, No. 4, pp. 411–428, 2007.
9. Yoshida, T., Senjyu, T., Nakamura, M., Yona, A., Urasak, N., and Sekine, H., "Position control of ultrasonic motor using two-control inputs H_∞ controller," *Elec. Power Comp. Syst.*, Vol. 35, No. 7, pp. 741–755, 2007.
10. Polycarpou, M. M., "Learning and convergence analysis of neural-type structure network," *IEEE Trans. Neural Networks*, Vol. 3, No. 1, pp. 39–50, 1992.